research articles Journal of proteome research

A P_4-ATPase Protein Interaction Network Reveals a Link between Aminophospholipid Transport and Phosphoinositide Metabolism

Catheleyne F. Puts,[†] Guillaume Lenoir,[†,‡] Jeroen Krijgsveld,[#,¶] Patrick Williamson,[§] and Joost C. M. Holthuis*[,†]

Membrane Enzymology, Bijvoet Center and Institute of Biomembranes, and Biomolecular Mass Spectometry and Proteomics Group, Bijvoet Center and Netherlands Proteomics Center, Utrecht University, 3584 CH Utrecht, The Netherlands and Department of Biology, Amherst College, Amherst, Massachusetts 01002

Received August 20, 2009

High-throughput analysis of protein−protein interactions can provide unprecedented insight into how cellular processes are integrated at the molecular level. Yet membrane proteins are often overlooked in these studies owing to their hydrophobic nature and low abundance. Here we used a proteomics-based strategy with the specific intention of identifying membrane-associated protein complexes. One important aspect of our approach is the use of chemical cross-linking to capture transient and low-affinity protein interactions that occur in living cells prior to cell lysis. We applied this method to identify binding partners of the yeast Golgi P_4-ATPase Drs2p, a member of a conserved family of putative aminophospholipid transporters. Drs2p was endogeneously tagged with both a polyhistidine and a biotinylation peptide, allowing tandem-affinity purification of Drs2p-containing protein complexes under highly stringent conditions. Mass-spectrometric analysis of isolated complexes yielded one known and nine novel Drs2p binding partners. Binding specificity was verified by an orthogonal *in vivo* membrane protein interaction assay, confirming the efficacy of our method. Strikingly, three of the novel Drs2p interactors are involved in phosphoinositide metabolism. One of these, the phosphatidylinositol-4-phosphatase Sac1p, also displays genetic interactions with Drs2p. Together, these findings suggest that aminophospholipid transport and phosphoinositide metabolism are interconnected at the Golgi.

Keywords: Split-ubiquitin assay • aminophospholipid translocase • Drs2p • P-type ATPase • phosphoinositide metabolism • membrane protein complex • mass spectrometry • *in vivo* cross-linking • Golgi • vesicle biogenesis

Introduction

Proteins rarely function in isolation; rather, they operate in macromolecular complexes that both carry out and integrate cellular processes.[1] Current approaches for mapping protein−protein interactions on a proteome-wide scale include tandem-affinity purification (TAP) of protein complexes followed by identification of individual components using mass spectrometry.[2,3] While these approaches are very effective in reducing nonspecific background, they cannot effectively capture weak or transient protein interactions. In this respect, identification of interaction networks involving integral membrane proteins is particularly challenging. Solubilization of membrane proteins requires the use of detergents, which may disrupt low affinity interactions and induce nonspecific ones.[4,5] Moreover, detection of integral membrane proteins by mass spectrometry is hampered by their overall low abundance, resistance to proteolytic cleavage, and relative high content of uncharged, hydrophobic residues. As a result, membrane proteins are largely underrepresented in studies analyzing protein interaction networks, even though they represent one-third of the proteome and nearly two-thirds of all known drug targets.[6]

Chemical cross-linking can be used to freeze protein−protein interactions by introducing covalent bonds between proteins while they are still in their native cellular environment.[7,8] In principle, cross-linked protein complexes can remain intact during cell lysis and then survive purification under highly stringent conditions. Guerrero et al.[9] recently developed an integrated approach using *in vivo* cross-linking of protein complexes combined with TAP under denaturing conditions to allow identification of weak and/or transient protein−protein interactions. This strategy has been used successfully to map the yeast 26S proteasome interaction network, employing histidine-biotin-histidine (HBH)-tagged proteasome subunits as baits.[9,10] *In vivo* cross-linking may overcome the inherent difficulty associated with preserving the integrity of low affinity interactions with native protein complexes embedded in cellular membranes. However, the potential of chemical cross-

* Corresponding author: Membrane Enzymology, Bijvoet Center and Institute of Biomembranes, Padualaan 8, 3584 CH Utrecht, The Netherlands. Phone, +31-30-253 6630; fax, +31-30-252 2478; e-mail, j.c.holthuis@uu.nl.
† Bijvoet Center and Institute of Biomembranes.
¶ Current address: CNRS, URA 2096 (Systèmes membranaires, photobiologie, stress et détoxication) and CEA, iBiTecS (Institut de Biologie et Technologie de Saclay), F-91191 Gif sur Yvette Cedex, France.
‡ Bijvoet Center and Netherlands Proteomics Center.
§ Current address: EMBL, Meyerhofstrasse 1, 69117 Heidelberg, Germany.
# Amherst College.

10.1021/pr900743b

Published on Web 12/08/2009

linking combined with TAP under highly stringent conditions for mapping the interaction network of low-abundance integral membrane proteins remains to be explored.

The P-type ATPases are a large family of polytopic membrane pumps characterized by transient autophosphorylation at a conserved aspartate residue as part of the reaction cycle. While P-type ATPases usually pump small cations or metal ions, members of the P_4 subfamily of P-type ATPases form a notable exception. P_4-ATPases are required for transbilayer phospholipid transport and are believed to create aminophospholipid asymmetry across membranes of the late secretory pathway.[11,12] The P_4-ATPase Drs2p resides primarily in the *trans*-Golgi network (TGN) of yeast and is essential for a flippase activity present in purified TGN membranes with specificity for phosphatidylserine (PS) and phosphatidylethanolamine (PE).[13,14] P_4-ATPases Dnf1p and Dnf2p are mainly found in the yeast plasma membrane, where they are required for transport of PC, and contribute to the transport of PE and PS.[15] P_4-ATPases form specific complexes with members of the Cdc50 family of membrane proteins. For example, Cdc50p associates with Drs2p, whereas Dnf1p and Dnf2p associate with Lem3p.[16] The recent finding that Cdc50p serves a vital role in the transport cycle of Drs2p indicates that Cdc50 subunits are integral components of the P_4-ATPase flippase machinery.[17] Proteoliposomes containing purified Drs2p−Cdc50p complexes display NBD-PS translocation activity,[18] indicating that P_4-ATPases associated with their Cdc50 binding partners form the minimal flippase unit. Whether P_4-ATPases require additional subunits for catalyzing efficient lipid transport is unclear.

P_4-ATPases also play an essential role in membrane trafficking between the Golgi and plasma membrane.[19,20] For instance, loss of Dnf1p and Dnf2p causes a cold-induced defect in the formation of endocytic vesicles at the plasma membrane.[15] Moreover, inactivation of Drs2p rapidly blocks formation of a clathrin-dependent class of post-Golgi secretory vesicles carrying exocytic cargo to the cell surface.[21] Two models have been proposed to explain how P_4-ATPases may contribute to vesicle formation. One possibility is that P_4-ATPases recruit coat proteins to the membrane through protein−protein interactions and/or by increasing the concentration of aminophospholipids in the cytosolic leaflet.[20,22] While this idea is consistent with the finding that Drs2p physically interacts with Arf activator Gea2p and clathrin adaptor protein AP-1, recruitment of AP-1 and clathrin to the TGN has been shown to occur independently of Drs2p.[23,24] An alternative possibility is that the physical displacement of aminophospholipid from the luminal to the cytosolic leaflet catalyzed by P_4-ATPases bends the membrane toward the cytosol, and in this way assists the coat machinery during vesicle budding.[20,22] How P_4-ATPases cooperate with coat proteins in vesicle biogenesis remains to be established.

To gain further insight into the mechanistic and biological functions of P_4-ATPases, we set out to map the protein interaction network of the yeast P_4-ATPase Drs2p. To this end, Drs2p was endogenously tagged with a polyhistidine and biotinylation peptide and subjected to *in vivo* cross-linking with formaldehyde. Cells expressing untagged Drs2p served as controls. Drs2p complexes were isolated by TAP under highly denaturing conditions. Mass-spectrometric analysis of isolated complexes yielded one known (i.e., Cdc50p) and nine novel Drs2p binding partners, including three enzymes involved in phosphoinositide metabolism, two of which were only captured after cross-linking. The authenticity of Drs2p binding partners was confirmed using a methodologically independent *in vivo* membrane protein interaction assay. Our findings demonstrate that TAP combined with *in vivo* cross-linking is a valuable approach to map the interaction networks of low-abundance membrane proteins and uncover an unexpected link between aminophospholipid transport and phosphoinositide metabolism with potential relevance for vesicle budding at the TGN.

Experimental Section

Yeast Strains. Yeast strains used for TAP of Drs2p complexes were isogenic to JHY074 (*sec6-4, TPI1::SUC2::TRP1, ura3-52 his3-Δ200 leu2-3−112 trp1-1 MAT*α). Strains used for the split-ubiquitin assay were THY.AP4 (*MATa ura3 leu2 lexA::lacZ::trp1 lexA::HIS3 lexA::ADE2*) and THY.AP5 (*MAT*α *ura3 leu2 trp1 his3 loxP::ade2*). All strains were grown in synthetic defined (SD) minimal media.

Assembly of HAH-Tag and pBirA Expression Construct. The HAH (3HA-Avi-10His) tag for PCR-based gene tagging in yeast was assembled as follows. An EcoR1/Hind3 fragment from pFA6a-HIS3MX[25] containing three copies of the HA epitope and the *HIS5* gene from *Schizosaccharomyces pombe* was ligated into EcoR1/Hind3-digested pBluescript II SK−, yielding p3XHAt-HIS5. A DNA fragment coding for the 15-residue Avi peptide (GLNDIFEAQKIEWHE) followed by a 10-residue long histidine tail and stop codon was created by primer extension and PCR amplification using pHusion DNA polymerase (Finnzymes, Espoo, Finland). The Avi-10His-STOP DNA fragment was inserted immediately downstream of the triple HA-tag in p3XHA-HIS5 by fusion PCR and DNA ligation, yielding p3XHA-Avi-10XHIS-HIS5. The open reading frame of *Escherichia coli* biotin ligase BirA was PCR amplified from pJMR1[26] (kindly provided by Christine Jaxel, CEA Saclay, France) and ligated behind the *PMA1* promoter into EcoR1/Not1-digested pRS426,[27] yielding pBirA.

HAH-Tagging and Cross-Linking. Drs2p was HAH-tagged at its carboxy terminus at the chromosomal locus using the PCR knock-in approach[25] and plasmid p3XHA-Avi-10XHIS-HIS5. Expression of tagged Drs2p was verified by immunoblotting using rabbit antibodies against Drs2p (kindly provided by T. Graham, Vanderbilt University, Nashville, TN) and the HA epitope (Santa Cruz Biotechnology, Santa Cruz, CA). For chemical cross-linking, $Drs2p^{HAH}$-expressing yeast (strain CPY033) was grown to $A_{600} = 1.2$ and then incubated with 1% formaldehyde (added from a 20% formaldehyde stock in PBS, pH 7.2) in SD medium at 30 °C for the indicated time period while shaking. Cross-linking was quenched by addition of 125 mM glycine for 5 min at 30 °C. Cells were collected by centrifugation ($500g_{av}$, 10 min, 4 °C), washed in ice-cold water and then washed again in ice-cold TES buffer (50 mM Tris-HCl, pH 7.5, 1 mM EDTA, 0.6 M sorbitol, 1 mM benzamidine, 1 mM PMSF, 1 μg/mL apoprotein, 1 μg/mL leupeptin, 1 μg/mL pepstatin and 5 μg/mL antipain) before storage at −80 °C.

Tandem-Affinity Purification of HAH-Tagged Drs2p. The $Drs2p^{HAH}$-expressing yeast strain (CPY033) was transformed with pBirA and then grown to $A_{600} = 1.2$ in uracil-deficient SD medium supplemented with 10 nM biotin. *In vivo* cross-linking was performed as described above. Cells were resuspended at 100 A_{600}/mL in ice-cold TES buffer and then lysed with glass beads by vortexing 10−15 times for 30 s with intermittent cooling on ice. The lysate was cleared by centrifugation at $700g_{av}$ (5 min, 4 °C). Membranes were collected by centrifugation at 100 000g_{av} (1 h, 4 °C) and solubilized in DDM buffer (0.5% dodecyl-β-D-maltoside, 100 mM NaCl, 20% glycerol, 5

mM imidazole, and 5 mM $MgCl_2$ supplemented with protease inhibitors) at a final protein concentration of 2 mg/mL on a rotating wheel for 2 h at 4 °C. Insoluble material was removed by centrifugation at 100 000g_{av} (1 h, 4 °C). The supernatant was mixed with Ni^{2+}-NTA sepharose (Amersham Biosciences) using 25 μL of a 50% slurry/mg of protein and then incubated on a rotating wheel for 4 h at 4 °C. The sepharose was washed at room temperature in 20 bed volumes of buffer A (8 M urea, 300 mM NaCl, 0.5% DDM, 50 mM NaH_2PO_4, pH 8.0); 20 bed volumes of buffer A at pH 6.3; and 20 bed volumes of buffer A at pH 6.3 containing 20 mM imidazole. Proteins were eluted in 3 × 1 bed volume of buffer B (8 M urea, 200 mM NaCl, 50 mM NaH_2PO_4, 2% SDS, 10 mM EDTA, 100 mM Tris, pH 4.3). The eluate was adjusted to pH 8.0 with 100 mM Tris and then loaded onto immobilized streptavidin beads (Pierce) pre-equilibrated in buffer B at pH 8.0 using 10 μL of a 50% slurry/mg of protein present in the crude membrane extract. After incubation overnight at room temperature, the streptavidin beads were washed in 25 bed volumes each of buffer C (8 M urea, 200 mM NaCl, 2% SDS, 100 mM Tris-HCl, pH 8.0); buffer D (8 M urea, 1.2 M NaCl, 0.2% SDS, 10% ethanol, 10% isopropanol, 100 mM Tris-HCl, pH 8.0); buffer E (8 M urea, 200 mM NaCl, 0.2% SDS, 10% ethanol, 10% isopropanol, 100 mM Tris-HCl, pH 5.0); buffer F (8 M urea, 200 mM NaCl, 0.2% SDS, 10% ethanol, 10% isopropanol, 100 mM Tris, pH 9.0); and buffer G (8 M urea, 100 mM Tris-HCl, pH 8.0). Finally, the beads were washed extensively with 100 mM Tris-HCl, pH 8.0, prior to trypsin digestion and mass spectrometric analysis.

LC-MS/MS. Proteins captured on streptavidin beads were subjected to on-bead Lys-C/trypsin digestion essentially as described in Guerrero et al.[9] Lys-C/trypsin digests were desalted using Stage-tips (50), and analyzed on a nanoflow LC-MS/MS system using a LTQ ion trap mass spectrometer (Thermo Electron, Bremen) operated as described.[51] All MS/MS spectra were converted to single DTA files using Bioworks 3.1 (Thermo) with default parameters, and merged into a file in Mascot generic format. This was searched against the yeast SGD database (5779 entries, obtained from http://www.yeastgenome.org, June 2007) using a Mascot search engine (version 2.2.03). Cysteine carbamidomethylation was used as a fixed modification; methionine oxidation and deamidation (at Asn and Gln) were chosen as a variable modification. A mass tolerance of 0.6 Da were used for both precursor and fragment masses, and Trypsin was chosen as proteolytic enzyme allowing one missed cleavage. All data were loaded into Scaffold (version 02.01.00, Proteome-Software, Portland, OR) to probabilistically validate peptide and protein identifications. Peptide and protein identifications were accepted when reaching a minimum of 95% probability, requiring a minimum of two peptides per protein.

Split-Ubiquitin Assay. The mating-based split-ubiquitin assay of Obrdlik et al.[28] was used. Proteins fusions with the C-terminus of ubiquitin (Cub) were constructed in yeast strain THY.AP4 by *in vivo* recombination between the linearized single copy vector pMETYCgate and PCR fragments, which were generated with pHusion DNA polymerase using yeast genomic DNA as template and the primer sets listed in Supplemental Table 1. Protein fusions with the N-terminus of ubiquitin (Nub) were made in yeast strain THY.AP5 by *in vivo* recombination between the linearized low copy vector pNXgate33-3HA or pXNgate-3HA and PCR fragments, which were generated as above. Interaction assays were carried out beginning with matings between Cub and Nub strains on SD plates, which were then replicated on SD-Leu-Trp plates to select for diploids. The diploids were then replicated on SD-Leu-Trp-His-Ade plates to test for growth. Sensitivity of these growth assays was determined by methionine (Meth) controlled expression of the Cub construct. Growth assays were carried out on plates containing 150 μM Meth. For quantitative assays of β-galactosidase expression, diploids were grown overnight in SD-Leu-Trp suspension cultures at 30 °C to an A_{600} between 0.5 and 1.2. One A_{600} of each culture was centrifuged, permeabilized in 100 μL of YPER permeabilization reagent (Pierce Chemical, Rockford, IL) for 20 min at room temperature, and then combined with 1 mL of Z buffer (60 mM Na_2HPO_4, 40 mM NaH_2PO_4, 10 mM KCl, 1 mM $MgSO_4$, pH 7.0) containing 4 mg/mL freshly added *o*-nitrophenyl-β-D-galactopyranoside (ONPG). After incubation at 30 °C for 10 min, the assay mixture was sedimented, and the A_{420} of the supernatant was measured to obtain specific activity for β-galactosidase.

Results

Strategy for the Identification of Drs2p Binding Partners. To identify novel binding partners of the yeast P_4 ATPase Drs2p, we used a modified version of the strategy developed by Guerrero et al.[9] for the purification of chemically cross-linked protein complexes (Figure 1). As a first step, we created a novel tandem-affinity (HAH) tag. The HAH tag consists of a triple HA epitope (3×HA) for immunodetection of tagged protein, a 15-residue Avitag peptide (Avi; GLNDIFEAQKIEWHE) and a polyhistidine sequence (10×His; Figure 1A). The 3-kDa HAH tag is much smaller than the 6×His-Bio-6×His (HBH) tag used for mapping the yeast 26S proteasome interaction network (20 kDa; ref 9), and therefore less likely to interfere with functionality. The Avitag serves as an *in vivo* recognition signal for the *E. coli* biotin ligase BirA that links biotin to a key lysine residue in position 10 of the peptide.[29] When coexpressed with BirA, HAH-tagged Drs2p can be sequentially purified by Ni^{2+} chelate chromatography and binding to streptavidin resin.

As both binding of a polyhistidine sequence to Ni^{2+} chelating resin and biotin to streptavidin tolerate extremely stringent washing conditions (e.g., 8 M urea, 4% SDS), we reasoned that combining these two steps would greatly facilitate the purification of low-abundance, polytopic membrane proteins such as Drs2p (10 membrane spans, ~600 molecules per cell).[30] The high affinity between biotin and streptavidin hampers efficient elution of HAH-tagged proteins from streptavidin beads. However, this does not pose a problem for mass spectrometric analysis because trypsin digestion is efficient on bead-bound proteins while streptavidin itself is largely resistant to trypsin digestion.[31] Prior to cell lysis, half of the culture was subjected to *in vivo* formaldehyde cross-linking to capture also transient and low affinity Drs2p interaction partners (Figure 1D). Next, cellular membranes were collected and solubilized in dodecyl-β-D-maltoside (DDM), a detergent that proved very effective in extracting Drs2p.[17] Drs2p protein complexes were isolated from DDM extracts by Ni^{2+} chelate chromatography and immobilized on streptavidin beads under highly denaturing conditions (8 M urea, 2% SDS). The purified complexes were digested with trypsin, and their composition was analyzed by LC-MS/MS for protein identification.

HAH-Tagged Drs2p Is Functional and Can Be Efficiently Biotinylated. Drs2p was HAH tagged at its carboxy terminus at the chromosomal locus so that endogenous levels of the tagged protein were expressed. Expression of HAH-tagged Drs2p ($Drs2p^{HAH}$) was verified by immunoblotting using anti-

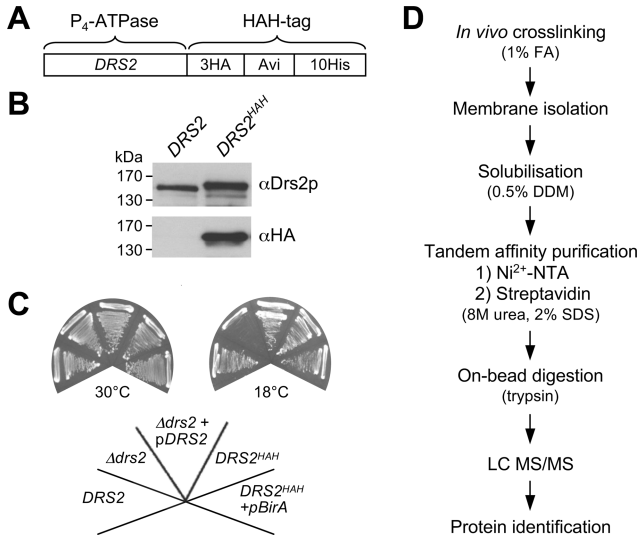

Figure 1. Strategy for the identification of novel binding partners of the yeast P_4-ATPase Drs2p. (A) HAH tag for tandem-affinity purification of Drs2p. The tag consists of three copies of the HA epitope (3HA) for immuno-detection, a 15 amino acid-residue Avitag peptide (Avi) for *in vivo* biotinylation by *E. coli* biotin ligase BirA, and a polyhistidine peptide (10His) for binding to Ni^{2+}-NTA resin. (B) Immunoblots of membrane extracts of yeast cells expressing untagged (*DRS2*) or HAH-tagged *DRS2* (*DRS2^{HAH}*) were stained with anti-Drs2p and anti-HA antibodies. (C) Wild-type (*DRS2*), *drs2* null mutant (Δ*drs2*) or *DRS2^{HAH}*-expressing yeast cells (*DRS2^{HAH}*) transfected with *DRS2* (+p*DRS2*) or biotin ligase BirA (+p*BirA*) were streaked out onto SD plates and then incubated at the indicated temperature for 4 days. (D) Schematic outline of the strategy. After *in vivo* cross-linking with formaldehyde, yeast cells coexpressing HAH-tagged Drs2p and BirA are lysed. Membranes collected by ultracentrifugation are solubilized using dodecyl-D-maltoside (DDM). Cross-linked, $Drs2p^{HAH}$ protein complexes are sequentially purified by Ni^{2+}-NTA chromatography and binding to streptavidin agarose beads under fully denaturing conditions (8 M Urea, 2% SDS). Peptides released after on-bead digestion with trypsin are analyzed by LC-MS/MS to identify Drs2p binding partners.

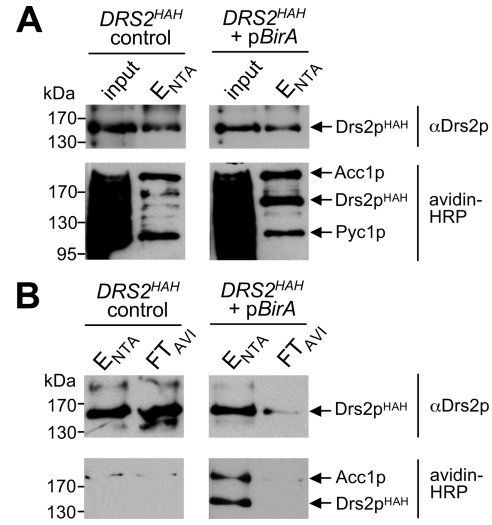

Figure 2. Tandem-affinity purification of HAH-tagged Drs2p. (A) Drs2p with a carboxy-terminal HAH tag was expressed from the chromosomal locus of a control strain (*DRS2^{HAH}* control) or a strain transfected with biotin ligase BirA (*DRS2^{HAH}* + p*BirA*) and then purified by Ni^{2+}-NTA chromatography. Aliquots of the solubilized membrane fraction (input) and Ni^{2+}-NTA eluate (E_{NTA}) were immunoblotted and stained with anti-Drs2p antibody (αDrs2p) or horseradish peroxidase-conjugated streptavidin (avidin-HRP). Note that biotinylated $Drs2p^{HAH}$ was only detectable in the strain expressing BirA. The endogenous biotinylated proteins Acc1p and Pyc1p are much more abundant than Drs2p so that their detection with avidin-HRP produced the major bands. (B) Ni^{2+}-NTA eluates of (A) were passed over streptavidin agarose beads to capture biotinylated $Drs2p^{HAH}$. Aliquots of the Ni^{2+}-NTA eluate (E_{NTA}) and the flow-through of streptavidin agarose (FT_{AVI}) were immunoblotted and stained with αDrs2p antibody or avidin-HRP. Note that $Drs2p^{HAH}$ purified from the BirA-expressing strain, but not from the control, was efficiently retained on streptavidin agarose, indicating that the bulk was biotinylated by BirA.

HA and anti-Drs2p antibodies. HAH tagging results in a mass increase of ~3 kDa, which can be observed as a slight decrease in mobility during SDS-PAGE (Figure 1B). HAH-tagging did not interfere with Drs2p function, since cells expressing only $Drs2p^{HAH}$ lacked the cold-sensitive growth phenotype of Δ*drs2* mutant cells (Figure 1C). Unlike Δ*drs2* mutant cells, cells expressing $Drs2p^{HAH}$ were also fully resistant to PE-binding peptide cinnamycin (data not shown). Resistance to low temperature and cinnamycin was also retained after heterologous expression of biotin ligase BirA, indicating that biotinylation of $Drs2p^{HAH}$ does not perturb its functionality (Figure 1C; data not shown).

We first tested the efficiency of biotinylation and purification of $Drs2p^{HAH}$ in the absence of formaldehyde cross-linking. Two strains were used, one expressing $Drs2p^{HAH}$ and the other coexpressing both $Drs2p^{HAH}$ and BirA. Membranes from these cells were solubilized in 0.5% DDM and incubated with Ni^{2+}-NTA resin. The resin was washed extensively under denaturing conditions (8 M urea, 0.5% SDS) and then $Drs2p^{HAH}$ was eluted with a buffer that disrupts interaction of the polyhistidine sequence with the Ni^{2+}-NTA resin (8 M urea, 2% SDS, 10 mM EDTA, pH 4.3). Immunoblot analysis of the Ni^{2+}-NTA eluate showed that >70% of $Drs2p^{HAH}$ was recovered following binding and elution from the resin (Figure 2A upper panel; data not shown). Probing these blots with horseradish peroxidase-conjugated streptavidin (avidin-HRP) showed that the eluate of the BirA-expressing strain contained biotinylated $Drs2p^{HAH}$ whereas the eluate of the control strain did not (Figure 2A, lower panel). While the first purification step by Ni^{2+} chelate chromatography removed the bulk of the endogenously biotinylated yeast proteins Acc1p (205 kDa), Pyc1/2p (120 kDa) and Arc1p (45 kDa), residual contamination by these proteins was sufficient to be visualized in the $Drs2p^{HAH}$-containing eluate (Figure 2A, lower panel; not shown for Arc1p).

After readjusting the pH to 8.0, the Ni^{2+}-NTA eluates were incubated with streptavidin-agarose. Immunoblot analysis showed that $Drs2p^{HAH}$ isolated from the control strain was fully recovered in the flow-through. In contrast, over 90% of $Drs2p^{HAH}$ isolated from the BirA-expressing strain was retained on the streptavidin resin (Figure 2B), demonstrating that *in vivo* biotinylation of $Drs2p^{HAH}$ by BirA is highly efficient.

Purification of *in vivo* Cross-Linked Drs2p Protein Complexes. To capture low affinity and transient Drs2p binding partners, yeast cells coexpressing $Drs2p^{HAH}$ and BirA were treated with the cross-linking reagent formaldehyde prior to tandem-affinity purification. Formaldehyde cross-links amino and imino groups between residues (mostly lysines) that are in close physical proximity (~2 Å).[32] To determine optimal

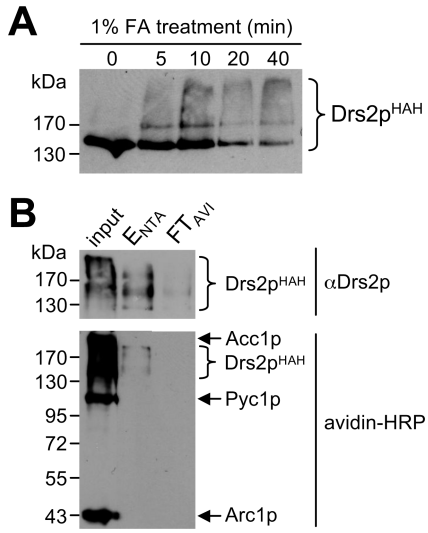

Figure 3. Tandem-affinity purification of cross-linked Drs2p^{HAH}protein complexes. (A) Yeast cells expressing Drs2p^{HAH} were incubated with 1% formaldehyde for the indicated time period at 30 °C and then subjected to immunblotting using αDrs2p antibody. (B) Tandem-affinity purification of Drs2p^{HAH} from a BirA-expressing strain after *in vivo* cross-linking with 1% formaldehyde for 15 min. Aliquots of the solubilized membrane fraction (input), the Ni^{2+}-NTA eluate (E_{NTA}) and the flow-through of streptavidin agarose (FT_{AVI}) were immunoblotted and stained with αDrs2p antibody or avidin-HRP.

cross-linking conditions, cells were incubated with 1% formaldehyde at 30 °C for different time periods. Cross-linking efficiency was monitored by immunoblot analysis. High molecular weight, cross-linked, Drs2p^{HAH}-containing protein complexes were formed within 5 min of incubation (Figure 3A). At an incubation time of 20 min or longer, there was a substantial (>70%) drop in the total recovery of Drs2p^{HAH} and its cross-linked adducts, suggesting that prolonged incubation with formaldehyde nonspecifically links proteins to insoluble material (e.g., chromatin) that is lost when the lysate is cleared by low speed centrifugation. Alternatively, neutralization of large numbers of basic groups by formaldehyde cross-linking may result in protein precipitation. We chose 15 min as the incubation time for all subsequent cross-linking experiments.

We also evaluated the effect of cross-linking on the efficiency of purification of Drs2p^{HAH}-containing protein complexes. Semiquantitative immunoblot analysis showed that ≥65% of untreated or cross-linked Drs2p^{HAH} could be bound to the Ni^{2+}-NTA resin, and that at least 90% of this material could be eluted (Figures 2B and 3B; data not shown). Moreover, the bulk (∼85%) of Drs2p^{HAH}-containing complexes in the Ni^{2+}-NTA eluate (E_{NTA}) could be captured on streptavidin beads. Together, these results demonstrate that cross-linking does not interfere with purification of Drs2p^{HAH}.

Identification of Drs2p Binding Partners. After optimizing the cross-linking and tandem-affinity purification conditions, we next analyzed Drs2p complexes isolated from a strain coexpressing Drs2p^{HAH} and BirA. The effect of *in vivo* cross-linking on the composition of Drs2p^{HAH}-containing complexes was determined by comparison with tandem-affinity purification from the same strain without prior cross-linking. In both cases, we used a preparation from a wild-type strain expressing untagged Drs2p as control for background proteins that bind Ni^{2+}-NTA and streptavidin resin independently of Drs2p. An example of the latter are the endogenously biotinylated proteins Acc1p, Pyc1/2p and Arc1p. As noted above, residual amounts of these proteins were present in Ni^{2+}-NTA eluates of wild-type and Drs2p^{HAH}-expressing strains, and so they were routinely captured on the streptavidin resin.

Proteins retained on the streptavidin resin were digested by trypsin and analyzed by LC-MS/MS. Table 1 lists all proteins captured specifically from the Drs2p^{HAH}-expressing strain; the corresponding peptides identified by LC-MS/MS are listed in Supplemental Table 2. Proteins also captured from the wild-type strain were excluded. Besides the biotinylated proteins Acc1p, Pyc1/2p, and Arc1p, background proteins included the mitochondrial proteins (Ilv5p, Por1p) and translation machinery components (Rpl3p, Rpl28p, Tef2p; Supplemental Table 3). Cross-linking caused a substantial rise in the number of background proteins and allowed the recovery of several previously identified binding partners of Acc1p (i.e., Hsc82p), Pyc1/2p (i.e., Rpl40p) and Arc1p (i.e., Gus1p, Etf2p, Hsc82p).

The known Drs2p-binding partner, Cdc50p, was among the proteins captured specifically from the Drs2p^{HAH}-expressing strain. In addition, we identified nine novel interactors with Drs2p. Four of these were transmembrane proteins (Sac1p, Itr1p, Tcb3p and Vnx1p), four others were cytosolic proteins (Ino1p, Sec26p, Mhp1p and Ssd1p), and one was a resident of the ER lumen (Kar2p/BIP). Some of the binding partners were found only after cross-linking (i.e., Sac1p, Ino1p and Kar2p), while others were captured regardless of cross-linking (Cdc50p and Sec26p). A third group was captured only without prior cross-linking (Itr1p, Tcb3p, Vnx1p, Ssd1p and Mhp1p). The latter two groups seem to represent interactions that are strong enough to resist tandem-affinity purification under denaturing conditions.

Validation of Drs2p Binding Partners. Remarkably, three of the newly identified putative interactors of Drs2p are proteins involved in phosphoinositide metabolism, namely, phosphatidylinositol-4-phosphatase Sac1p, *myo*-inositol transporter Itr1p, and *myo*-inositol 1-phosphate synthase Ino1p (Table 1). Other binding partners include the synaptotagmin orthologue Tcb3p, COPI β-subunit Sec26p, cation/H^+ antiporter Vnx1p, TOR pathway component Ssd1p, ER chaperone Kar2p/BIP, and microtubule-associated protein Mhp1p. From these, we selected all integral membrane proteins and proteins involved in phosphoinositide metabolism (i.e., Sac1p, Itr1p, Ino1p, Tcb3p and Vnx1p) for validation of their interactions with Drs2p by an independent method. To this end, we employed the split-ubiquitin assay, a method for monitoring membrane protein interactions *in vivo*.[28,33] When two proteins carrying the C-terminal "Cub" and N-terminal "Nub" halves of ubiquitin interact, a complete ubiquitin can be formed. This results in the proteolytic release of a transcription factor that activates reporter genes required for growth on selective media and for expression of β-galactosidase, whose activity can be measured quantitatively.

As shown in Figure 4A, an interaction between Drs2p and Cdc50p can be detected by the growth assay when Cub and Nub moieties are fused to the C-terminus of Drs2p and the N-terminus of Cdc50p, respectively. This interaction is specific, as a similar interaction was not observed with two other tagged Cdc50 family members, Nub-Lem3 and Nub-Crf1. Conversely, Nub-Lem3 and Nub-Crf1 showed specific interactions with the Cub-tagged P_4 ATPases Dnf1 and Dnf3, respectively (Figure 4A). These results were confirmed by quantitative measurements of β-galactosidase activity (Figure 4C) and show that each P_4-

Table 1. Identified Drs2p Binding Partners[a]

ID	function	localization	MW	no. TMD	no. molecules per cell*	no. unique peptides found − FA	no. unique peptides found + FA	SUS verified
Drs2p	P_4 ATPase transporter	Golgi (PM)	153834	10	606	36	17	NA
Cdc50p	P_4 ATPase β subunit	Golgi (PM)	44967	2	589	1	3	+
Sac1p	PI_4P phosphatase	ER/Golgi	71108	2	48,000	0	3	+
Ino1p	Inositol 1-phosphate synthase	Cytosol	59626	0	unknown	0	2	+
Itr1p	Myo-inositol transporter	PM	63553	12	unknown	2	0	+
Tcb3p	Synaptotagmin orthologue	PM	171063	1	4,280	11	0	+
Vnx1p	Cation/H^+ antiporter	Vacuole	102498	13	259	3	0	+
Ssd1p	TOR pathway component	Cytosol	139940	0	1,100	2	0	ND
Kar2p	BIP/chaperone	ER	74467	0	337,000	0	3	ND
Sec26p	COPI β subunit	Cytosol	109006	0	26,000	5	2	ND
Mhp1p	Microtubule-associated protein	Cytosol	155193	0	279	4	0	ND

[a] Summary of proteins identified by LC MS/MS as components of native (−FA) or *in vivo* cross-linked (+FA) Drs2p^{HAH} complexes purified by TAP. *Numbers based on a global analysis of protein expression in yeast.[29] ID, identity; MW, molecular weight; TMD, transmembrane domain; SUS, split-ubiquitin system; NA, not applicable; ND, not determined; FA, formaldehyde; PM, plasma membrane; ER, endoplasmic reticulum.

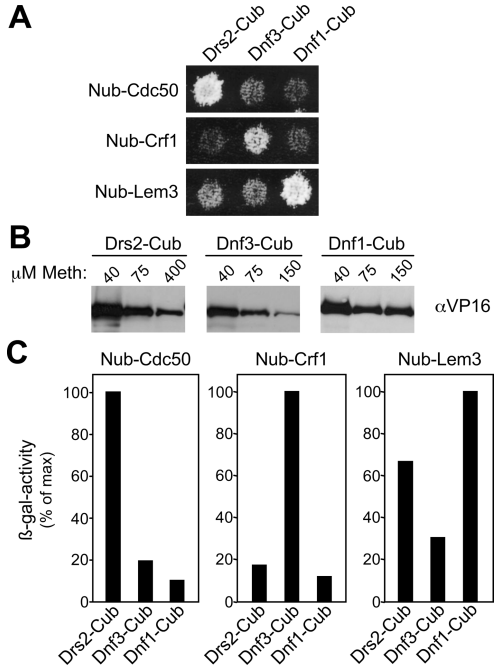

Figure 4. Split-ubiquitin assay showing interactions between P_4-ATPases and their cognate Cdc50 subunits. (A) Split-ubiquitin growth assay reporting interactions of Drs2-Cub, Dnf3-Cub and Dnf1-Cub and their Cdc50 binding partners Nub-Cdc50, Nub-Crf1 and Nub-Lem3. (B) Modulation of Cub fusion expression by varying the methionine (Meth) concentration in the medium. Membrane extracts from equal amounts of cells were immunoblotted using an antibody directed against the PLV moiety of the Cub fusion (αVP16). (C) Quantitative measurement of Nub-Cdc50, Nub-Crf1 and Nub-Lem3 interactions with P_4-ATPase-Cub fusions in cells grown in 75 μM Meth (Drs2-Cub, Dnf1-Cub) or 40 μM Meth (Dnf3-Cub) using the split-ubiquitin β-galactosidase assay. Specific β-galactosidase activity levels were expressed as percentage of the maximum level, with the 100% values corresponding to 2.39 (Nub-Cdc50), 2.12 (Nub-Crf1) and 2.30 U/mg protein (Nub-Lem3).

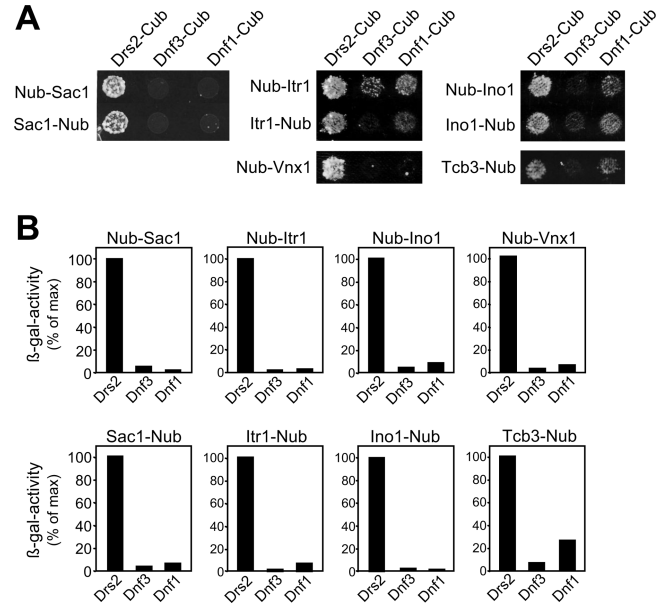

Figure 5. Validation of newly identified Drs2p binding partners by the split-ubiquitin assay. (A) Split-ubiquitin growth assay reporting interactions of Drs2-Cub, Dnf3-Cub and Dnf1-Cub with C- or N-terminal Nub-fusions of Sac1, Itr1, Ino1, Vnx1 and Tcb3. (B) Quantitative measurement of interactions of C- or N-terminal Nub-fusions of Sac1, Itr1, Ino1, Vnx1 and Tcb3 with P_4-ATPase-Cub fusions in cells grown at 75 μM Met (Drs2-Cub, Dnf1-Cub) or 40 μM Met (Dnf3-Cub) using the split-ubiquitin β-galactosidase assay. Specific β-galactosidase activity levels were expressed as percentage of the maximum level, with the 100% values corresponding to 1.11 (Nub-Sac1), 0.68 (Sac1-Nub), 1.45 (Nub-Itr1), 0.93 (Itr1-Nub), 1.57 (Nub-Ino1), 1.10 (Ino1-Nub), 0.88 (Nub-Vnx1), and 1.11 U/mg protein (Tcb3-Nub).

ATPase interacts with a different Cdc50 subunit *in vivo*, a conclusion consistent with coimmunoprecipitation analysis.[16,34] Importantly, these results demonstrate the suitability of the split-ubiquitin assay as an independent method to test the authenticity of the newly identified proteins as binding partners of Drs2p.

We then applied the split-ubiquitin assay to validate association of Drs2p with the five selected candidate binding partners. As shown in Figure 5A, an interaction between Drs2-Cub and Nub-tagged Sac1 was detected in the growth assay, regardless of whether the Nub moiety was fused to the N- or C-terminus of Sac1p. This interaction appears specific for Drs2p, since a similar interaction was not observed with the closely related P_4-ATPases Dnf3-Cub or Dnf1-Cub. While Dnf1p primarily resides at the plasma membrane, Drs2p and Dnf3p both localize in the *trans*-Golgi network,[15,19] indicating that the differences in interaction are not just the result of differences in the subcellular distribution of the transporters. Immuno-

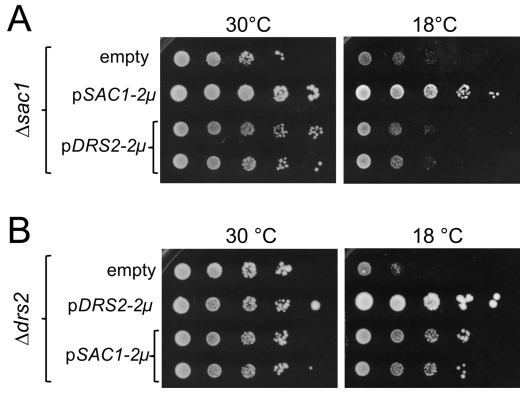

Figure 6. Drs2p and Sac1p interact genetically. (A) Serial dilutions of a Δ*sac1* mutant strain transfected with empty vector (empty), multicopy *SAC1* vector (*pSAC1-2* μ) or multicopy *DRS2* vector (*pDRS2−2* μ) were spotted onto SD plates and incubated at 30 or 18 °C for 4 d. (**B**) Serial dilutions of a Δ*drs2* mutant strain transfected with empty vector (empty), multicopy *DRS2* vector (*pDRS2−2* μ) or multicopy *SAC1* vector (*pSAC1−2*μ) were spotted onto SD plates and incubated as in (A).

blotting revealed that Dnf3-Cub was expressed at approximately 5-fold lower levels than Drs2-Cub or Dnf1-Cub, raising the possibility that the difference in apparent interaction might be a consequence of lower levels of Dnf3-Cub expression. This possibility could be tested because transcription of the Cub fusions is under the control of the Met promotor, and so their expression levels can be adjusted by varying the methionine concentration in the medium (Figure 4B). When methionine concentrations were adjusted to equalize P_4 ATPase-Cub expression levels, the level of β-galactosidase activity in cells expressing Nub-tagged Sac1 with Drs2-Cub was still much higher than in cells expressing Dnf3-Cub or Dnf1-Cub (Figure 5B). This result shows that the apparent preferential interaction between Drs2p and Sac1p is not an artifact of the expression levels of the Cub-tagged proteins. Similar results were obtained for Itr1p, Ino1p, Tcb3p and Vnx1p (Figure 5), confirming that these proteins form specific complexes with Drs2p. Together, this entirely independent method for detecting protein−protein interactions validates the majority of Drs2p interactors identified by our mass spectrometry approach (six out of six analyzed) as authentic binding partners of Drs2p.

Drs2p and Sac1p Display Genetic Interactions. Of all Drs2p binding partners identified, Sac1p is of particular interest. Like Drs2p, Sac1p has been reported to play a critical role in anterograde trafficking from the Golgi complex.[35−37] Loss of Drs2p causes a constitutive defect in the formation of one class of exocytic vesicles[21] and in an AP-1/clathrin-dependent pathway from the Golgi to early endosomes.[19] At temperatures of 20 °C or below, Δ*drs2* cells cease growth. This is likely due to a cold-sensitive defect in a Golgi-localized, γ-ear-containing Arf-binding protein (GGA)/clathrin-dependent pathway from the Golgi to the vacuole combined with the constitutive defect in the AP-1/clathrin pathway.[38] Sac1p has been proposed to negatively regulate a Golgi-associated pool of phosphatidylinositol-4-phosphate that is essential for anterograde trafficking.[36] As would be expected if this function antagonizes anterograde trafficking from the Golgi, loss of Sac1p partially restores growth in Δ*drs2* cells at 20 °C.[38] Curiously, at temperatures below 20 °C, cells lacking Sac1p also display a cold-sensitive growth phenotype (Figure 6A). While overexpression of Drs2p is unable to suppress the cold-sensitive growth phenotype in Δ*sac1* cells, we found that overexpression of Sac1p partially suppresses the corresponding phenotype in Δ*drs2* cells (Figure 6B). The demonstration that Drs2p and Sac1p display genetic interactions suggests that their physical interaction is functionally important for anterograde membrane trafficking from the Golgi.

Discussion

Studies of the protein interactome have so far been of limited value for identifying interactions involving integral membrane proteins, presumably because of the many technical artifacts introduced by the highly hydrophobic nature of these proteins. In this work, we applied a proteomics-based strategy to identify proteins that interact with a specific integral membrane protein, the yeast Golgi P_4-ATPase Drs2p. *In vivo* cross-linking was used in combination with tandem-affinity purification under stringent conditions to capture also transient and low affinity protein interactions that might be lost during conventional purification methods. This approach benefited from the previous identification of one integral membrane protein that specifically interacts with Drs2p, namely, Cdc50p. We could confidently predict that this protein should be identified in a stringent search for Drs2p binding partners. In fact, our approach led to the identification of this known protein and nine novel Drs2p binding partners, with half of them representing integral membrane proteins. Six of the identified binding partners were subjected to further analysis using an orthogonal *in vivo* membrane protein interaction assay, which confirmed them as authentic interactors with Drs2p. This group included two low-abundance proteins (fewer than 600 molecules per cell) with multiple membrane spans. Together, the data qualify our method as a valuable approach for elucidating the membrane protein interactome.

The term "Drs2p interactor" or "Drs2p binding partner" is hereby used for describing a protein that is either in direct physical contact with or in close spatial proximity of Drs2p by forming part of the same protein complex. While the total number of Drs2p binding partners identified appears rather high, it has been estimated that all major processes in cells are carried out by assemblies of 10 or more proteins.[1] It is unlikely that all of these proteins assemble into a single complex. Rather, the 9 newly identified Drs2p binding partners are more likely to be part of a heterogeneous population of Drs2p containing complexes. Although Drs2p primarily resides in the *trans*-Golgi network at steady state, we identified an ER-resident chaperone (i.e., Kar2p/BIP) as well as two plasma membrane proteins (i.e., Itr1p, Tcb3p) among its binding partners. The ER chaperone Kar2p/BIP presumably represents a transient and low affinity interactor that may assist in the correct assembly of the Drs2p/Cdc50p heterodimer, which is required for Drs2p export from the ER.[16] This model is consistent with the capture of Kar2p/BIP only after *in vivo* cross-linking with formaldehyde. We previously showed that Drs2p enters post-Golgi secretory vesicles.[14] This indicates that Drs2p is at least a transient occupant of the plasma membrane, which may account for its ability to interact with Itr1p and Tcb3p that are located there.

While our analysis reconfirmed Cdc50p as an authentic binding partner of Drs2p, it did not yield another known Drs2p interactor, Gea1p.[24] Formaldehyde cross-links lysine residues at ~2 Å distance, and it is entirely possible that some Drs2p interactors do not have lysine residues in close enough proximity to be captured by this method. Using cross-linkers with

longer spacer arms might overcome this problem. Because formaldehyde reacts primarily with lysines, its application should reduce the availability of trypsin cleavage sites and hence decrease the recovery of fragments for mass spectrometric analysis. This effect may explain why the number of unique peptides derived from Drs2p itself is substantially lower in the cross-linked sample as compared to the untreated sample, and why several Drs2p-binding partners were picked up only in the absence of cross-linker. Application of a reversible cross-linker may help prevent this drop in sensitivity. Nevertheless, three Drs2p binding partners were captured uniquely after cross-linking with formaldehyde (Kar2p/BIP, Ino1p, Sac1p). As indicated above for Kar2p/BIP, this behavior suggests that these proteins bind Drs2p only weakly or very transiently. Conversely, other interactors were identified regardless of cross-linking (Cdc50p, Sec26p) or only in the absence of cross-linker (Itr1p, Tcb3p, Vnx1p, Ssd1p, Mhp1p), indicating that their interaction with Drs2p is strong enough to survive highly denaturing conditions (8 M urea, 2% SDS). Together, our data indicate that the identification of both stable and transient interactors is best served by combining the analysis of samples with and without cross-linking.

The Drs2p binding partners identified in this study fall in different functional categories. The protein Mhp1p was described as a stabilizer of microtubules.[39] The movement of Drs2p-containing vesicles along microtubule tracks may bring Drs2p into proximity with this protein. Similarly, Sec26p corresponds to the β-subunit of COPI, which is involved in retrograde Golgi-to-ER membrane trafficking.[40] An association between Drs2p and Sec26p in the Golgi may account for this interaction. COPI subunits have been shown to physically interact with Sac1p,[41] suggesting that Sec26p might associate with Drs2p in a ternary complex with Sac1p. Tcb3p is a member of the tricalbin protein family. Tricalbins contain three C2 domains that show Ca^{2+}-dependent binding to phosphatidylserine and multiple phosphoinositides.[42] Because they are similar to synaptotagmin, it has been proposed that tricalbins may contribute to fusion-related events in membrane trafficking.[43] While the biological relevance of the interaction between Tcb3p and Drs2p is unclear, both proteins have previously been identified as components of a complex containing the putative flavin carrier Flc2p and the multidrug transporter homologue Pdr5p.[2]

Strikingly, three of the verified Drs2p binding partners (Ino1p, Itr1p and Sac1p) are proteins involved in phosphoinositide metabolism. The *myo*-inositol 1-phosphate synthase Ino1p catalyzes the rate-limiting step in the production of inositol phosphate, a precursor for the biosynthesis of phosphatidylinositol and its phosphorylated derivatives.[44,45] The other major route of inositol supply in yeast is uptake from the medium by the principal inositol transporter Itr1p.[46] Phosphatidylinositol is a direct precursor of phosphoinositol-containing sphingolipids, which are synthesized on the luminal aspect of the Golgi,[47] and sphingolipid biosynthesis is controlled, at least in part, by the supply of phosphatidylinositol.[48] As Drs2p corresponds to a prominent aminophospholipid transport activity in yeast,[13,14] its association with both Ino1p and Itr1p may be relevant for the establishment of a proper transbilayer lipid arrangement in membranes that pass through the Golgi complex on their way to the plasma membrane.

Sac1p is a member of the synaptojanin family of lipid phosphatases and predominantly acts as a phosphatidylinositol-4-phosphatase.[49] Sac1p antagonizes anterograde membrane trafficking from the Golgi by restricting the local pool of PI(4)P required for efficient recruitment of the vesicle budding machinery.[37,50] Drs2p facilitates vesicle formation independently of coat recruitment.[23] Instead, it has been proposed that translocation of aminophospholipid from the exoplasmic to the cytosolic leaflet by Drs2p induces membrane curvature, which is captured by coat proteins in vesicles.[20,23] An intriguing possibility is that a physical interaction between Drs2p and Sac1p may link flippase activity to coat recruitment as part of the properly organized segregation of cargo molecules into secretory vesicles. The recent observation that Drs2p-catalyzed flippase activity is stimulated by binding of PI(4)P to a regulatory domain in the C-terminal tail of the enzyme is fully consistent with this notion.[51] However, our finding that overexpression of Sac1p partially suppresses the cold-sensitive growth defect in Δ*drs2* cells suggests that the model of an antagonistic relationship between the two proteins is too simple.[38]

Conclusions

Our findings demonstrate that tandem-affinity purification of *in vivo* cross-linked protein complexes under strongly denaturing conditions can provide a snapshot of the interaction networks of low abundance integral membrane proteins. This approach allowed us to uncover a link between aminophospholipid transport and phosphoinositide metabolism with potential relevance for membrane maturation and vesicle biogenesis in the secretory pathway.

Abbreviations: Cub, C-terminal half of ubiquitin; DDM, dodecyl-β-D-maltoside; E_{NTA}, Ni-NTA eluate; HA, hemagglutinin; HAH, hemagglutinin-avidine-histidine; LC-MS/MS, liquid chromatography-tandem mass spectrometry; meth, methionine; Ni-NTA, nickel-nitrilotriacetic acid; Nub, N-terminal half of ubiquitin; ONPG, *o*-nitrophenyl-β-D-galactopyranoside; TAP, tandem affinity purification; TES, Tris-EDTA-sorbitol; TGN, *trans*-Golgi network; PE, phosphatidylethanolamine; PI(4)P, phosphatidylinositol-4-phosphate; PS, phosphatidylserine; SD,synthetic minimal medium; SDS, sodium dodecyl sulfate; TOR, target of rapamycin; YPER, yeast permeabilization reagens.

Acknowledgment. We thank Todd Graham, Peter Mayinger and Christine Jaxel for providing antibodies and DNA constructs. This work was supported by The Netherlands Proteomics Center and by grants from the Dutch Organization of Sciences (NWO-CW), the Utrecht High Potential Program (to J.H.), and the National Science Foundation (to P.W.).

Supporting Information Available: Supplemental Table 1, primer sets used for creation of Nub and Cub constructs. Supplemental Table 2, peptides identified from tandem-affinity purified $Drs2p^{HAH}$ protein complexes. Supplemental Table 3, proteins captured from untagged strain. This material is available free of charge via the Internet at http://pubs.acs.org.

References

(1) Alberts, B. The cell as a collection of protein machines: preparing the next generation of molecular biologists. *Cell* **1998**, *92* (3), 291–4.

(2) Gavin, A. C.; Bosche, M.; Krause, R.; Grandi, P.; Marzioch, M.; Bauer, A.; Schultz, J.; Rick, J. M.; Michon, A. M.; Cruciat, C. M.; Remor, M.; Hofert, C.; Schelder, M.; Brajenovic, M.; Ruffner, H.; Merino, A.; Klein, K.; Hudak, M.; Dickson, D.; Rudi, T.; Gnau, V.; Bauch, A.; Bastuck, S.; Huhse, B.; Leutwein, C.; Heurtier, M. A.;

Copley, R. R.; Edelmann, A.; Querfurth, E.; Rybin, V.; Drewes, G.; Raida, M.; Bouwmeester, T.; Bork, P.; Seraphin, B.; Kuster, B.; Neubauer, G.; Superti-Furga, G. Functional organization of the yeast proteome by systematic analysis of protein complexes. *Nature* **2002**, *415* (6868), 141–7.
(3) Gavin, A. C.; Aloy, P.]?>;]?>; Grandi, P.]?>;]?>; Krause, R.; Boesche, M.; Marzioch, M.; Rau, C.; Jensen, L. J.; Bastuck, S.; Dumpelfeld, B.; Edelmann, A.; Heurtier, M. A.; Hoffman, V.; Hoefert, C.; Klein, K.; Hudak, M.; Michon, A. M.; Schelder, M.; Schirle, M.; Remor, M.; Rudi, T.; Hooper, S.; Bauer, A.; Bouwmeester, T.; Casari, G.; Drewes, G.; Neubauer, G.; Rick, J. M.; Kuster, B.; Bork, P.; Russell, R. B.; Superti-Furga, G. Proteome survey reveals modularity of the yeast cell machinery. *Nature* **2006**, *440* (7084), 631–6.
(4) Rashid, K. A.; Hevi, S.; Chen, Y.; Le Caherec, F.; >Chuck, S. L. A proteomic approach identifies proteins in hepatocytes that bind nascent apolipoprotein B. *J. Biol. Chem.* **2002**, *277* (24), 22010–7.
(5) Seddon, A. M.; Curnow, P.; Booth, P. J. Membrane proteins, lipids and detergents: not just a soap opera. *Biochim. Biophys. Acta* **2004**, *1666* (1−2), 105–17.
(6) Yildirim, M. A.; Goh, K. I.; Cusick, M. E.; Barabasi, A. L.; Vidal, M. Drug-target network. *Nat. Biotechnol.* **2007**, *25* (10), 1119–26.
(7) Sinz, A. Chemical cross-linking and mass spectrometry to map three-dimensional protein structures and protein-protein interactions. *Mass Spectrom. Rev.* **2006**, *25* (4), 663–82.
(8) Zhang, H.; Tang, X.; Munske, G. R.; Tolic, N.; Anderson, G. A.; Bruce, J. E. Identification of protein-protein interactions and topologies in living cells with chemical cross-linking and mass spectrometry. *Mol. Cell. Proteomics* **2009**, *8* (3), 409–20.
(9) Guerrero, C.; Tagwerker, C.; Kaiser, P.; Huang, L. An integrated mass spectrometry-based proteomic approach: quantitative analysis of tandem affinity-purified in vivo cross-linked protein complexes (QTAX) to decipher the 26 S proteasome-interacting network. *Mol. Cell. Proteomics* **2006**, *5* (2), 366–78.
(10) Guerrero, C.; Milenkovic, T.; Przulj, N.; Kaiser, P.; Huang, L. Characterization of the proteasome interaction network using a QTAX-based tag-team strategy and protein interaction network analysis. *Proc. Natl. Acad. Sci. U.S.A.* **2008**, *105* (36), 13333–8.
(11) Lenoir, G.; Williamson, P.; Holthuis, J. C. On the origin of lipid asymmetry: the flip side of ion transport. *Curr. Opin. Chem. Biol.* **2007**, *11* (6), 654–61.
(12) Daleke, D. L. Phospholipid flippases. *J. Biol. Chem.* **2007**, *282* (2), 821–5.
(13) Natarajan, P.; Wang, J.; Hua, Z.; Graham, T. R. Drs2p-coupled aminophospholipid translocase activity in yeast Golgi membranes and relationship to in vivo function. *Proc. Natl. Acad. Sci. U.S.A.* **2004**, *101* (29), 10614–9.
(14) Alder-Baerens, N.; Lisman, Q.; Luong, L.; Pomorski, T.; Holthuis, J. C. Loss of P4 ATPases Drs2p and Dnf3p disrupts aminophospholipid transport and asymmetry in yeast post-Golgi secretory vesicles. *Mol. Biol. Cell* **2006**, *17* (4), 1632–42.
(15) Pomorski, T.; Lombardi, R.; Riezman, H.; Devaux, P. F.; van Meer, G.; Holthuis, J. C. Drs2p-related P-type ATPases Dnf1p and Dnf2p are required for phospholipid translocation across the yeast plasma membrane and serve a role in endocytosis. *Mol. Biol. Cell* **2003**, *14* (3), 1240–54.
(16) Saito, K.; Fujimura-Kamada, K.; Furuta, N.; Kato, U.; Umeda, M.; Tanaka, K. Cdc50p, a protein required for polarized growth, associates with the Drs2p P-type ATPase implicated in phospholipid translocation in Saccharomyces cerevisiae. *Mol. Biol. Cell* **2004**, *15* (7), 3418–32.
(17) Lenoir, G.; Williamson, P.; Puts, C. F.; Holthuis, J. C. Cdc50p plays a vital role in the ATPase reaction cycle of the putative aminophospholipid transporter drs2p. *J. Biol. Chem.* **2009**, *284* (27), 17956–67.
(18) Zhou, X.; Graham, T. R. Reconstitution of phospholipid translocase activity with purified Drs2p, a type-IV P-type ATPase from budding yeast. *Proc. Natl. Acad. Sci. U.S.A.* **2009**, *106* (39), 16586–91.
(19) Hua, Z.; Fatheddin, P.; Graham, T. R. An essential subfamily of Drs2p-related P-type ATPases is required for protein trafficking between Golgi complex and endosomal/vacuolar system. *Mol. Biol. Cell* **2002**, *13* (9), 3162–77.
(20) Graham, T. R. Flippases and vesicle-mediated protein transport. *Trends Cell Biol.* **2004**, *14* (12), 670–7.
(21) Gall, W. E.; Geething, N. C.; Hua, Z.; Ingram, M. F.; Liu, K.; Chen, S. I.; Graham, T. R. Drs2p-dependent formation of exocytic clathrin-coated vesicles in vivo. *Curr. Biol.* **2002**, *12* (18), 1623–7.
(22) Pomorski, T.; Holthuis, J. C.; Herrmann, A.; van Meer, G. Tracking down lipid flippases and their biological functions. *J. Cell Sci.* **2004**, *117* (Pt 6), 805–13.
(23) Liu, K.; Surendhran, K.; Nothwehr, S. F.; Graham, T. R. P4-ATPase requirement for AP-1/clathrin function in protein transport from the trans-Golgi network and early endosomes. *Mol. Biol. Cell* **2008**, *19* (8), 3526–35.
(24) Chantalat, S.; Park, S. K.; Hua, Z.; Liu, K.; Gobin, R.; Peyroche, A.; Rambourg, A.; Graham, T. R.; Jackson, C. L. The Arf activator Gea2p and the P-type ATPase Drs2p interact at the Golgi in Saccharomyces cerevisiae. *J. Cell Sci.* **2004**, *117* (5), 711–22.
(25) Wach, A.; Brachat, A.; Pohlmann, R.; Philippsen, P. New heterologous modules for classical or PCR-based gene disruptions in Saccharomyces cerevisiae. *Yeast* **1994**, *10* (13), 1793–808.
(26) Abbott, J.; Beckett, D. Cooperative binding of the *Escherichia coli* repressor of biotin biosynthesis to the biotin operator sequence. *Biochemistry* **1993**, *32* (37), 9649–56.
(27) Sikorski, R. S.; Hieter, P. A system of shuttle vectors and yeast host strains designed for efficient manipulation of DNA in Saccharomyces cerevisiae. *Genetics* **1989**, *122* (1), 19–27.
(28) Obrdlik, P.; El-Bakkoury, M.; Hamacher, T.; Cappellaro, C.; Vilarino, C.; Fleischer, C.; Ellerbrok, H.; Kamuzinzi, R.; Ledent, V.; Blaudez, D.; Sanders, D.; Revuelta, J. L.; Boles, E.; Andre, B.; Frommer, W. B. K+ channel interactions detected by a genetic system optimized for systematic studies of membrane protein interactions. *Proc. Natl. Acad. Sci. U.S.A.* **2004**, *101* (33), 12242–7.
(29) Athavankar, S.; Peterson, B. R. Control of gene expression with small molecules: biotin-mediated acylation of targeted lysine residues in recombinant yeast. *Chem. Biol.* **2003**, *10* (12), 1245–53.
(30) Ghaemmaghami, S.; Huh, W. K.; Bower, K.; Howson, R. W.; Belle, A.; Dephoure, N.; O'Shea, E. K.; Weissman, J. S. Global analysis of protein expression in yeast. *Nature* **2003**, *425* (6959), 737–41.
(31) Tagwerker, C.; Flick, K.; Cui, M.; Guerrero, C.; Dou, Y.; Auer, B.; Baldi, P.; Huang, L.; Kaiser, P. A tandem affinity tag for two-step purification under fully denaturing conditions: application in ubiquitin profiling and protein complex identification combined with in vivocross-linking. *Mol. Cell. Proteomics* **2006**, *5* (4), 737–48.
(32) Pomorski, T.; Menon, A. K. Lipid flippases and their biological functions. *Cell. Mol. Life Sci.* **2006**, *63* (24), 2908–21.
(33) Johnsson, N.; Varshavsky, A. Split ubiquitin as a sensor of protein interactions in vivo. *Proc. Natl. Acad. Sci. U.S.A.* **1994**, *91* (22), 10340–4.
(34) Furuta, N.; Fujimura-Kamada, K.; Saito, K.; Yamamoto, T.; Tanaka, K. Endocytic recycling in yeast is regulated by putative phospholipid translocases and the Ypt31p/32p-Rcy1p pathway. *Mol. Biol. Cell* **2007**, *18* (1), 295–312.
(35) Cleves, A. E.; Novick, P. J.; Bankaitis, V. A. Mutations in the SAC1 gene suppress defects in yeast Golgi and yeast actin function. *J. Cell Biol.* **1989**, *109* (6 Pt 1), 2939–50.
(36) Schorr, M.; Then, A.; Tahirovic, S.; Hug, N.; Mayinger, P. The phosphoinositide phosphatase Sac1p controls trafficking of the yeast Chs3p chitin synthase. *Curr. Biol.* **2001**, *11* (18), 1421–6.
(37) Blagoveshchenskaya, A.; Mayinger, P. SAC1 lipid phosphatase and growth control of the secretory pathway. *Mol. BioSyst* **2009**, *5* (1), 36–42.
(38) Muthusamy, B. P.; Raychaudhuri, S.; Natarajan, P.; Abe, F.; Liu, K.; Prinz, W. A.; Graham, T. R. Control of protein and sterol trafficking by antagonistic activities of a P4-ATPase and oxysterol binding protein homologue. *Mol. Biol. Cell* 2009.
(39) Irminger-Finger, I.; Hurt, E.; Roebuck, A.; Collart, M. A.; Edelstein, S. J. MHP1, an essential gene in Saccharomyces cerevisiae required for microtubule function. *J. Cell Biol.* **1996**, *135* (5), 1323–39.
(40) Letourneur, F.; Gaynor, E. C.; Hennecke, S.; Demolliere, C.; Duden, R.; Emr, S. D.; Riezman, H.; Cosson, P. Coatomer is essential for retrieval of dilysine-tagged proteins to the endoplasmic reticulum. *Cell* **1994**, *79* (7), 1199–207.
(41) Rohde, H. M.; Cheong, F. Y.; Konrad, G.; Paiha, K.; Mayinger, P.; Boehmelt, G. The human phosphatidylinositol phosphatase SAC1 interacts with the coatomer I complex. *J. Biol. Chem.* **2003**, *278,* (52), 52689–99.
(42) Schulz, T. A.; Creutz, C. E. The tricalbin C2 domains: lipid-binding properties of a novel, synaptotagmin-like yeast protein family. *Biochemistry* **2004**, *43* (13), 3987–95.
(43) Creutz, C. E.; Snyder, S. L.; Schulz, T. A. Characterization of the yeast tricalbins: membrane-bound multi-C2-domain proteins that form complexes involved in membrane trafficking. *Cell. Mol. Life Sci.* **2004**, *61,* (10), 1208–20.
(44) Majerus, P. W. Inositol phosphate biochemistry. *Annu. Rev. Biochem.* **1992**, *61,* 225–50.
(45) Gaspar, M. L.; Aregullin, M. A.; Jesch, S. A.; Henry, S. A. Inositol induces a profound alteration in the pattern and rate of synthesis and turnover of membrane lipids in Saccharomyces cerevisiae. *J. Biol. Chem.* **2006**, *281* (32), 22773–85.

(46) Nikawa, J.; Tsukagoshi, Y.; Yamashita, S. Isolation and characterization of two distinct myo-inositol transporter genes of Saccharomyces cerevisiae. *J. Biol. Chem.* **1991**, *266* (17), 11184–91.
(47) Levine, T. P.; Wiggins, C. A.; Munro, S. Inositol phosphorylceramide synthase is located in the Golgi apparatus of Saccharomyces cerevisiae. *Mol. Biol. Cell* **2000**, *11* (7), 2267–81.
(48) Brice, S. E.; Alford, C. W.; Cowart, L. A. Modulation of sphingolipid metabolism by the phosphatidylinositol-4-phosphate phosphatase Sac1p through regulation of phosphatidylinositol in Saccharomyces cerevisiae. *J. Biol. Chem.* **2009**, *284* (12), 7588–96.
(49) Konrad, G.; Schlecker, T.; Faulhammer, F.; Mayinger, P. Retention of the yeast Sac1p phosphatase in the endoplasmic reticulum causes distinct changes in cellular phosphoinositide levels and stimulates microsomal ATP transport. *J. Biol. Chem.* **2002**, *277* (12), 10547–54.
(50) Vicinanza, M.; D'Angelo, G.; Di Campli, A.; De Matteis, M. A. Function and dysfunction of the PI system in membrane trafficking. *EMBO J.* **2008**, *27* (19), 2457–70.
(51) Natarajan, P.; Liu, K.; Patil, D. V.; Sciorra, V. A.; Jackson, C. L.; Graham, T. R. Regulation of a Golgi flippase by phosphoinositides and an ArfGEF. *Nat. Cell Biol.* **2009**, *11* (12), 1421–6.

PR900743B